Journal of Directed Energy, 2, Spring 2007, 273–284

Incoherent Combining of High-Power Fiber Lasers for Long-Range Directed Energy Applications

Phillip Sprangle, Joseph Peñano,* Bahman Hafizi,[1] and Antonio Ting

Plasma Physics Division, Naval Research Laboratory, Washington, D.C. 20375

Coherent and incoherent fiber laser beam combining for long-range directed energy applications is discussed. We present a configuration for incoherently combining fiber lasers that can be employed for these applications. Unlike coherent beam combining approaches, incoherent combining does not require phase locking between the fiber lasers, and the polarization of the individual lasers can be random. In addition, the linewidths of the fiber lasers can be large. These relaxed requirements on the incoherent beam combining configuration allow for the use of recently developed high-continuous-wave (CW) power (~2.5 kW per fiber), single-mode (TEM_{00}), high-quality ($M^2 < 1.2$) fiber lasers having relatively large linewidths ($\delta\lambda/\lambda \sim 1\%$). These high-power lasers cannot be used for coherent beam combining. The proposed incoherent combining configuration consists of an array of fiber lasers in which the beams diffract to a spot size of ~4 cm onto individual collimating lenses. The Rayleigh length associated with each beam is ~5 km. The collimated beams can be directed to a target at distances of more than 5 km by individually controlled steering mirrors that form the beam director. We present parameters for an incoherently combined high-energy laser system that can deliver 100 kW of CW power on a target of area 100 cm^2 at a range of 5 km. The system has 49 fiber lasers and a beam director with transverse dimension 60 × 60 cm. In principle, this configuration is scalable to higher CW powers. The effects of atmospheric turbulence on the propagation efficiency are addressed for the incoherent beam combining configuration.

KEYWORDS: Atmospheric propagation, High-power fiber laser, Incoherent beam combining

1. Introduction

Recent advances in fiber lasers have made them a leading candidate for directed energy (DE) applications. Advantages of high-power fiber lasers for DE applications include i) high wall plug efficiency (>25%), ii) high continuous-wave (CW) power (~2.5 kW), iii) single-mode operation (TEM_{00}), iv) good beam quality ($M^2 < 1.2$), v) compactness (0.3 m^3/kW), vi) satisfactory wavelength ($\lambda = 1.075\ \mu m$),[9] vii) low cooling requirements, viii) low maintenance, ix) long life (diode life >10,000 h), and x) low operating cost.[4,11] The main cost limit for CW fiber laser power is the pump diodes.

Received July 17, 2006; revision received April 6, 2007.

*Corresponding author; e-mail: joseph.penano@nrl.navy.mil.

[1]Icarus Research, Inc., Bethesda, MD 20824-0780.

To achieve the power levels needed for DE applications (>100 kW, CW), it is necessary to combine a large number of them for efficient propagation over distances of many kilometers (>5 km). Fiber lasers can be combined spectrally,[10] coherently,[2,3,8,13] or incoherently. In this paper we discuss some of the issues associated with coherent and incoherent beam combining and propose an incoherent beam combining configuration for long-range DE applications. The propagation efficiency, defined as the ratio of the power incident on a target of a given area to the transmitted power, is the main metric used in this study to evaluate the various beam combining techniques.

Coherent beam combining relies on constructive interference of many lasers to produce high intensities on a remote target. It requires precise phase locking of the fiber lasers, polarization matching, very narrow linewidths ($\delta\lambda/\lambda < 10^{-6}$), and good optical beam quality. These requirements are difficult to achieve in practice and limit the individual fiber laser power to <400 W. The propagation efficiency for coherent combining is also limited by the filling factor of the fiber array, i.e., a low filling factor results in a significant amount of optical energy in lobes outside of the central lobe. To date, only a small number of fiber lasers have been coherently combined and at power levels far below that required for DE applications. The most recent experiments report that four fiber lasers were coherently combined to produce a total power of ~470 W (Ref. 13). The state of the art in single-mode, single-fiber lasers having a well-defined polarization is <400 W (Ref. 5). Although spectral beam combining is not discussed here, it should be mentioned that recently three fiber lasers were spectrally combined, resulting in a single-mode beam with $M^2 \sim 1.2$ and a total power of 522 W (Ref. 6).

Incoherent beam combining, on the other hand, does not require phase locking, polarization matching, or narrow linewidths. Because of these relaxed conditions, recently developed high-CW-power fiber lasers can be used. These fiber lasers can produce ~2.5 kW of CW power in a single mode (TEM_{00}) with high beam quality. For example, at the 2005 CLEO/Europe meeting, IPG Photonics reported[4] CW powers of 2 kW at a wavelength of $\lambda = 1.075$ μm from a ytterbium fiber laser. The fiber laser operated in a single mode, (TEM_{00}), and had excellent beam quality, $M^2 < 1.2$. Because of the large linewidths (~1%) and random polarization, these lasers cannot, however, be used for coherent combining.

Coherent beam combining requires over an order of magnitude more fibers than incoherent beam combining for the same power on target. This is due to the lower power per fiber and lower propagation efficiency associated with the coherent combining configuration.

In the following sections, we present examples of coherently and incoherently combined laser systems, both designed to deliver 100 kW of CW power on target. In Sec. 2 we present an example of a coherently combined laser system and indicate some of the issues and limitations of this configuration. Section 3 presents an example of our proposed incoherent beam combining configuration and examines the effect of tilt errors on both the coherent and incoherent systems. Section 4 addresses the effects of atmospheric turbulence on the propagation of the incoherently combined beams. Finally, we conclude with a discussion of a near-term, 20-kW, long-range demonstration experiment and indicate that the configuration, in principle, can scale to higher power (500 kW).

2. Coherent Beam Combining

Coherent beam combining uses an array of many phase-locked fibers to extend the diffraction length by increasing the effective spot size of the combined transmitted beam. Coherent beam combining requires that the phases and polarizations of the fiber lasers be

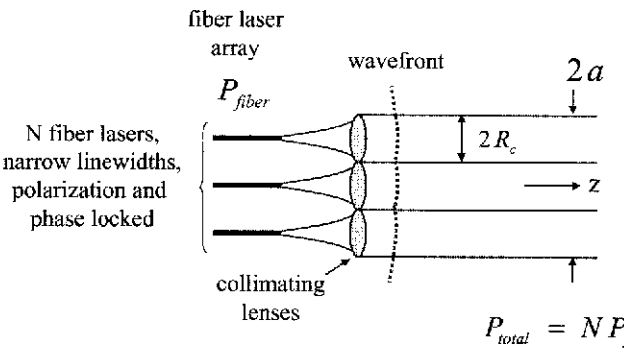

Fig. 1. Schematic of a coherently combined fiber array producing a uniform wavefront at the output. The individual lasers are Gaussian (TEM_{00}) modes with a spot size R_0. Each laser is passed through a collimating lens of radius R_C. The total transmitted power is NP_{fiber}, and the array dimension is $a \sim N^{1/2}R_C$.

matched.[5,12] The effective diffraction length of the fiber array is $Z_{\text{coherent}} \approx N\pi R_0^2/\lambda$, where N is the number of coherently combined lasers, R_0 is the spot size of an individual collimated beam, and λ is the wavelength, as shown in Fig. 1. Perfectly coherently combined beams can extend the diffraction length in the absence of turbulence by a factor of N. However, for a given power per fiber P_{fiber}, the total transmitted power is NP_{fiber}, which is the same as for incoherent combining. Furthermore, even if the individual beams are perfectly phase matched, the transverse intensity profile is highly non-Gaussian. The interference pattern in the far field consists of a central lobe and side lobes. The side lobes contain a significant amount of energy and have larger spreading angles. For the case in which the transverse intensity profile is uniform, the diffraction or spreading angle is $\Theta = \lambda/2a$ $(0.61\lambda/R_0)$ for a square (circular) transverse cross section. The potential for a smaller size beam director in the coherent combining configuration may be offset by thermal blooming near the beam director.[9]

In the following illustration of coherent beam combining, we simulate the propagation of 625 beams from a fiber array that delivers 100 kW of CW power to a 100-cm^2-area target at a distance of 5 km. We assume that each fiber laser has a power of 400 W and is perfectly phase and polarization matched. The total transmitted power is 250 kW, and the propagation efficiency is $\eta = 40\%$.

Each individual laser beam is assumed to be a collimated Gaussian (TEM_{00}) mode with a spot size of $R_0 = 1$ mm at the collimating lens. Note that the small spot size at the lens makes it difficult in practice to implement phase locking because of thermal deformation. The fibers are arranged in a square array with nearest neighbors separated by a distance of $2R_C = 3.3$ mm, where R_C is the radius of the collimating lens.

Figure 2 shows the transverse laser intensity profile as a function of propagation distance for the coherently combined array. Figure 2a shows the intensity at the beam director ($z = 0$). Figure 2b shows the interference pattern of the intensity in the near field ($z = 0.5$ km), which is defined by $z \ll \pi a^2/\lambda \approx 5$ km. Figure 2c shows the emergence of a central Gaussian lobe surrounded by side lobes. The side lobes represent higher order modes that have large diffraction angles and can contain a significant fraction of the total beam energy. In the far-field limit (Fig. 2d), the side lobes are located far from the central lobe and the central lobe

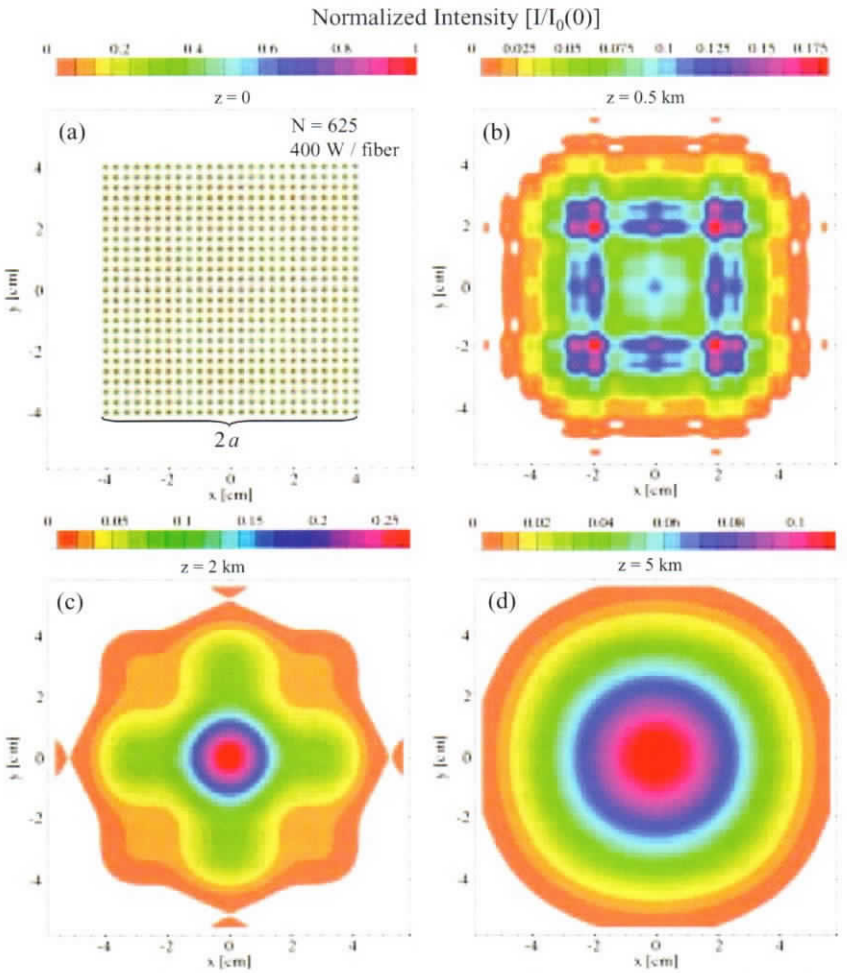

Fig. 2. Fiber array for coherent beam combining: (a) laser intensity profile at the beam director for 625 fibers; x and y denote transverse coordinates. Intensity is normalized to $I_0(0)$, which denotes the on-axis intensity at $z = 0$. The Gaussian spot size of each laser is 1 mm. The individual lasers are separated by $2R_C = 3.3$ mm. The size of the array is $a = 4$ cm, and the power per fiber is assumed to be $P_{\text{fiber}} = 400$ W. The total transmitted power is 250 kW. Panels (b), (c), and (d) show the intensity profile at $z = 0.5$, 2, and 5 km, respectively. The power on target is 100 kW for a target with a circular area of $A_{\text{target}} = 100$ cm^2 at a range of $L = 5$ km.

has diffracted such that its spot size is comparable to the target dimension. The dashed curve in Fig. 3 shows the spatial profile of the laser intensity in the target plane ($L = 5$ km). The solid curve in Fig. 3 represents the fractional power contained within a given radius. There is a well-defined central lobe with a radius approximately equal to the target radius. However, the central lobe contains only ~35% of the laser energy. In this beam director configuration, approximately 65% of the energy is in the higher order modes, which propagate at larger

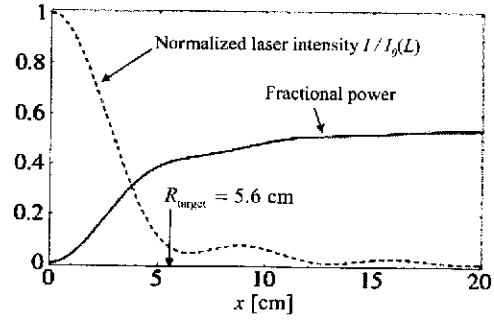

Fig. 3. Fractional power (solid curve) and normalized laser intensity (dashed curve) versus transverse coordinate x at a range of $L = 5$ km for the coherent beam director of Fig. 2. Fractional power is defined as the power contained within a circle of radius x normalized to the total transmitted power. The radius of a circular target with an area of 100 cm^2 is $R_{\text{target}} = 5.6$ cm. Laser intensity is normalized to $I_0(L) = 2.8$ kW/cm^2, which denotes the on-axis laser intensity at $z = L$. The power on target is 100 kW.

diffraction angles. The propagation efficiency is a function of the array's filling factor and can be slightly larger if the beams are arranged in a hexagonal pattern.

Sensitivity to spatial and angular errors is important in all laser beam combining configurations. A limitation on the coherent combining case is the tilt angle error associated with the N fibers. To avoid smearing the phases of the N lasers, the rms value of the tilt angle error $\delta\theta_{\text{rms}}$ must satisfy the smaller of the inequalities, $\delta\theta_{\text{rms}} < \lambda/a \sim 10$ μrad or $\delta\theta_{\text{rms}} < (2\lambda/L)^{1/2} \sim 14$ μrad. Examples with tilt error are presented in the following section.

3. Incoherent Beam Combining

For incoherent beam combining, the spot size of the individual lasers at the source is made large enough so that each individual beam does not diffract significantly over the propagation range. Each beam is then directed to the target by an individually controlled steering mirror. The schematic for the incoherent beam combining configuration is shown in Fig. 4. For this configuration, the design and operation of the steering mirrors is critical for the combining of the individual fiber lasers onto a distant target. A number of other beam director configurations also can be employed for incoherent combining, e.g., a class of Cassegrain or zoom lens-type of beam director.

Incoherent combining is readily analyzed using Hermite–Gaussian or Laguerre–Gaussian optics. The spot size of a collimated beam, e.g., from a single fiber, propagating in free space, is given by $R(z) = R_0[1 + (z/Z_R)^2]^{1/2}$, where $Z_R = \pi R_0^2/(M^2\lambda)$ is the Rayleigh length, R_0 is the spot size at the source ($z = 0$), and M^2 is the "times diffraction limited" beam quality. The radius of the collimating lens needed to illuminate a target having an area of $A_{\text{target}} = \pi R_{\text{target}}^2$ at a range L is

$$R_C = \alpha R_{\text{target}}\left\{1 + \left[1 - (M^2\lambda L)^2/(\pi R_{\text{target}}^2)^2\right]^{1/2}\right\},$$

where $\alpha \equiv R_C/R_0$ is related to the lens collecting efficiency, i.e., $\eta_C = 1 - \exp(-2\alpha^2) = 94\%$ for $\alpha = 1.2$, and $(M^2\lambda L)^2/(\pi R_{\text{target}}^2)^2 < 1$. In the case in which the collimating lenses *focus* the individual beams on the target, the lens radius is $R_C = \alpha M^2(\lambda/\pi R_{\text{target}})L$.

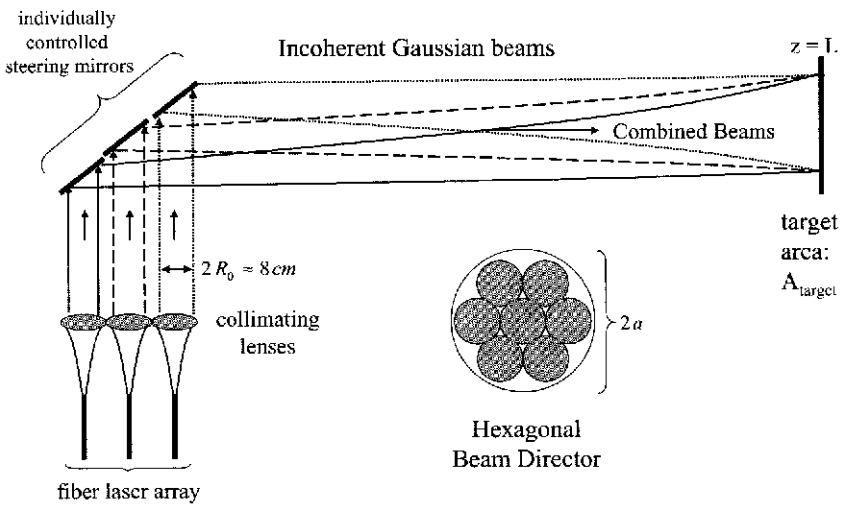

Fig. 4. Schematic of incoherent beam combining configuration. The individual lasers are Gaussian (TEM_{00}) modes. From the fiber, each laser diffracts to a spot size $R_0 \sim 4$ cm and passes through a collimating lens of radius $R_C = 1.2R_0$. Individually controlled steering mirrors direct each beam to the target. To minimize diffractive spreading, the range to the target must be $<2Z_R$, where $Z_R = \pi R_0^2/\lambda = 5$ km is the Rayleigh length associated with the individual beams. The total transmitted power is NP_{fiber}, and the beam director array dimension is $a \sim \sqrt{N}R_C$. An example of a hexagonal array of seven fibers is also shown.

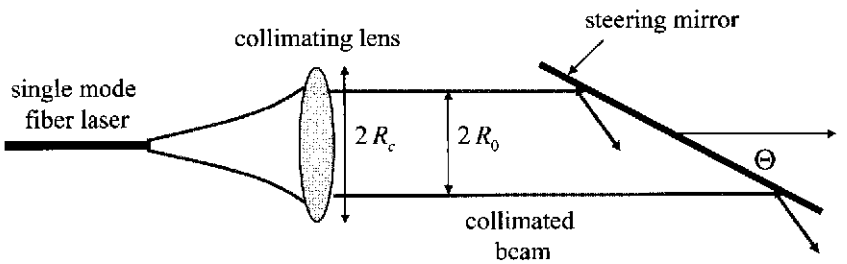

Fig. 5. Expanded diagram of a single-fiber laser system used in the incoherent beam combining configuration of Fig. 4. The individual lasers are Gaussian (TEM_{00}) modes. The laser from the fiber diffracts to a spot size $R_0 \sim 4$ cm and passes through a collimating lens of radius $R_C = 1.2\ R_0$. A steering mirror directs the beam to the target. The steering mirror angle Θ is defined with respect to the propagation axis and may have a tilt error denoted by the rms value $\delta\theta_{\text{rms}} \ll 1$.

As an example we take the target to have a range of $L = 5$ km and a cross-sectional area of $A_{\text{target}} = 100\ \text{cm}^2$ ($R_{\text{target}} = 5.6$ cm). The fiber laser wavelength is $\lambda = 1.075\ \mu$m, the CW power of each fiber is 2.5 kW, and the beam quality is $M^2 = 1.1$. In this example the radius of the collimating lens is $R_C = 4.8$ cm.

Figure 5 shows a single-fiber laser system used in the incoherent beam combining configuration. The beam exiting the fiber has a spot size of $\sim 20\ \mu$m and a Rayleigh length of ~ 1.5 mm. Hence, it requires ~ 2 m of propagation for the spot size to expand to ~ 4 cm to

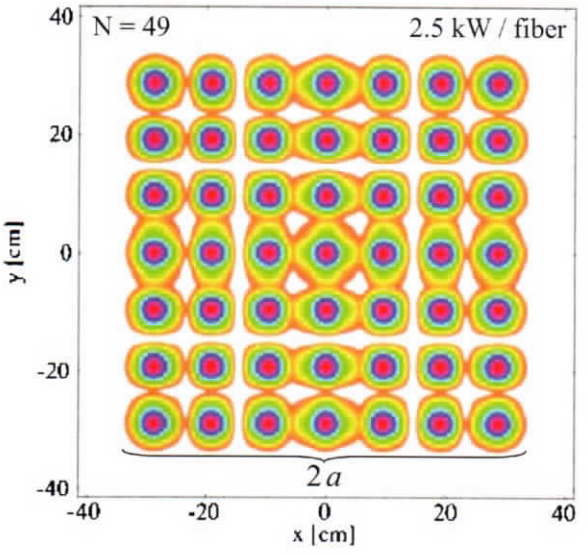

Fig. 6. Fiber array for incoherent beam combining, showing laser intensity profile at the beam director ($z = 0$) for 49 fibers arranged in a square array. The Gaussian spot size of each laser is 4 cm. The individual lasers are separated by 9.6 cm. The size of the array is $a = 33$ cm, and the power per fiber is taken to be $P_{\text{fiber}} = 2.5$ kW. The total transmitted power is 123 kW. The power on target is 100 kW for a target with a circular area of $A_{\text{target}} = 100\ \text{cm}^2$ at a range of $L = 5$ km.

efficiently cover the collimating lens. The beam then propagates to a steering mirror that directs the beam to the target. To maintain a high propagation efficiency, the rms angular tilt angle error associated with the individual steering mirrors must satisfy the inequality $\delta\theta_{\text{rms}} < R_{\text{target}}/L$, which is $\sim 10\ \mu$rad in this incoherent beam combining example.

Taking the number of fibers to be $N = 49$, the total transmitted CW power is $P_T = NP_{\text{fiber}} = 123$ kW. The beam director is taken to have a square transverse profile of dimension $\sim 60 \times 60$ cm. Figure 6 shows the laser intensity profile at the source. Each beam is given an initial linewidth of $\sim 1\%$ and a random phase. The beams remain Gaussian as they propagate to the target. The intensity of each beam is given by $I(r, z) = I_0 \exp[-2r^2/R^2(z)]R_0^2/R^2(z)$. The total power on target for incoherent combining is

$$P_{\text{target}} = N \int_0^{R_{\text{target}}} I(r, L) 2\pi r \mathrm{d}r = NP_{\text{fiber}}\left\{1 - \exp\left[-2R_{\text{target}}^2/R^2(L)\right]\right\}.$$

The propagation efficiency is defined as the ratio of the power incident on a target of a given area to the transmitted power. Figure 7 shows that the average laser intensity in the target plane (dashed curve) has a Gaussian profile. The spot size of the beam is comparable to the size of the target, but unlike in the coherent beam combining example, the propagation efficiency is twice as large ($\sim 81\%$).

Figure 8 plots the propagation efficiency versus rms tilt error $\delta\theta_{\text{rms}}$ for both coherent (dashed curve) and incoherent (solid curve) beam combining. The propagation efficiency, for both cases, decreases with increasing tilt error by a similar amount. For $\delta\theta_{\text{rms}} = 10\ \mu$rad,

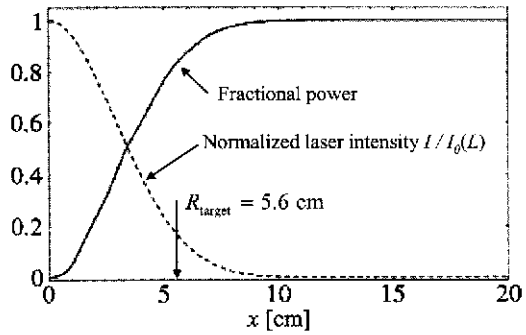

Fig. 7. Fractional power (solid curve) and normalized laser intensity (dashed curve) versus transverse coordinate x at a range of $L = 5$ km for the incoherent beam director of Fig. 6. Fractional power is defined as the power contained within a circle of radius x normalized to the total transmitted power. The radius of a circular target with an area of 100 cm^2 is $R_{target} = 5.6$ cm. Laser intensity is normalized to $I_0(L) = 2.2$ kW/cm^2, which denotes the on-axis laser intensity at $z = L$. The power on target is 100 kW.

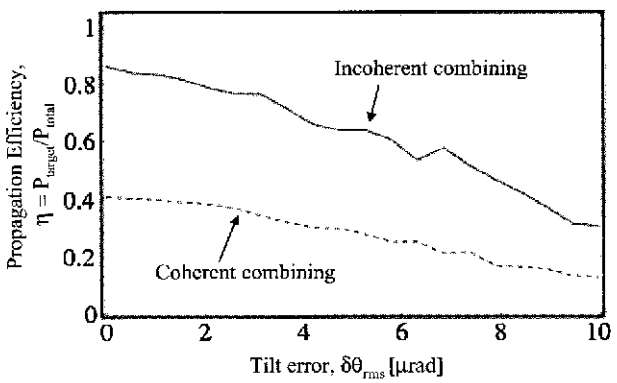

Fig. 8. Propagation efficiency $\eta = P_{target}/P_{total}$ versus rms tilt error $\delta\theta_{rms}$ for the coherent (dashed curve) and incoherent (solid curve) beam combining examples of Figs. 2 and 6. Propagation efficiency is defined as the ratio of the power on target to the transmitted power. The target is taken to have a circular area of $A_{target} = 100$ cm^2 at a range of $L = 5$ km. Each laser is given a random tilt error relative to the propagation axis with rms value $\delta\theta_{rms}$.

both the coherent and incoherent propagation efficiencies are reduced by a factor of ~3 relative to the case of zero tilt error.

4. Effects of Atmospheric Turbulence

In this section we address the effects of atmospheric turbulence on the incoherent beam combining configuration. Propagation through atmospheric turbulence results in spreading and wandering of the beam radius and fluctuations of the laser intensity on the target, i.e., scintillation. Turbulence is modeled by a Kolmogorov distribution, with the strength of the turbulence characterized by the structure function parameter C_n^2 (Ref. 1).

For a laser beam in the absence of jitter and thermal blooming effects, the longtime beam radius (including beam wander and spreading) is given by

$$R(L) = R_0\left[\left(1 - \frac{L}{L_f}\right)^2 + \left(\frac{\lambda L}{\pi R_0^2}\right)^2\left(M^4 + \frac{2R_0^2}{\rho_0^2}\right)\right]^{1/2},$$

where R_0 is the initial spot size, L_f is the focal length, and ρ_0 is the transverse coherence length. This equation is appropriate for near-Gaussian beams ($M^2 \sim 1$) but becomes less accurate when $M^2 > 1$ because of the coupling of higher order modes with turbulence. For a collimated beam, $L_f \gg L$ and L_f is positive (negative) in the case of a focused (defocused) beam. For a constant turbulence parameter C_n^2, the coherence length is

$$\rho_0 = 0.158\left(\frac{\lambda^2}{C_n^2 L}\right)^{3/5}.$$

Note that the Fried parameter is equal to $2.1\rho_0$. In the present example, $C_n^2 = 10^{-15}$ m$^{-2/3}$, $L = 5$ km, $\lambda = 1$ μm, and the transverse coherence length is found to be $\rho_0 \approx 6.6$ cm. For a collimated beam with initial spot size $R_0 = 4$ cm, the beam radius expands to $R = 5.6$ cm due to diffraction and turbulence ($C_n^2 = 10^{-15}$ m$^{-2/3}$) increases it to $R = 6.6$ cm at the range $L = 5$ km.

Scintillations represent a temporal intensity fluctuation that has an average statistical value. The normalized laser intensity variance is defined by

$$\sigma_I^2 = \frac{\langle (I - \langle I \rangle)^2 \rangle}{\langle I \rangle^2} = \frac{\delta I_{\text{rms}}^2}{\langle I \rangle^2},$$

where I is the instantaneous intensity on axis, $\langle I \rangle$ is the time-averaged intensity on axis, and δI_{rms} is the rms intensity fluctuation on axis. For a collimated laser beam and constant C_n^2 the intensity variance is

$$\sigma_I^2 \approx 10.5(L/\lambda)^{7/6} L^{2/3} C_n^2.$$

Using the parameters in this example, we find that the normalized intensity variance is $\sigma_I^2 = 0.63$ and the rms intensity fluctuation on target is

$$\delta I_{\text{rms}} = \sigma_I \langle I \rangle \approx 0.8 \langle I \rangle.$$

The atmospheric laser propagation code HELCAP is used to simulate the propagation of the laser beams from the fiber array of Fig. 6 to the target. HELCAP is a three-dimensional, fully time-dependent, nonlinear atmospheric propagation code, the details of which are discussed in Ref. 9. Atmospheric turbulence is modeled in the standard way using phase screens distributed along the propagation path that modify the phase of the laser beam.[7] The phase perturbations on each screen are characterized by a Kolmogorov spectrum with a strength parameter C_n^2. In the simulations that follow, we use 10 phase screens along the propagation path.

Figure 9 shows the average intensity profile in the target plane for a case of no turbulence (Fig. 9a), weak turbulence,[1] i.e., $C_n^2 = 10^{-15}$ m$^{-2/3}$ (Fig. 9b), and moderate turbulence, i.e., $C_n^2 = 5 \times 10^{-15}$ m$^{-2/3}$ (Fig. 9c) for the fiber array example of Fig. 6. Figure 10 shows the fractional power curves corresponding to the three cases shown in Fig. 9. In the absence of turbulence, the propagation efficiency for a 100-cm^2 target at $L = 5$ km is ~81%. For $C_n^2 = 10^{-15}$, and 5×10^{-15} m$^{-2/3}$, the propagation efficiency is ~60% and ~35%, respectively.

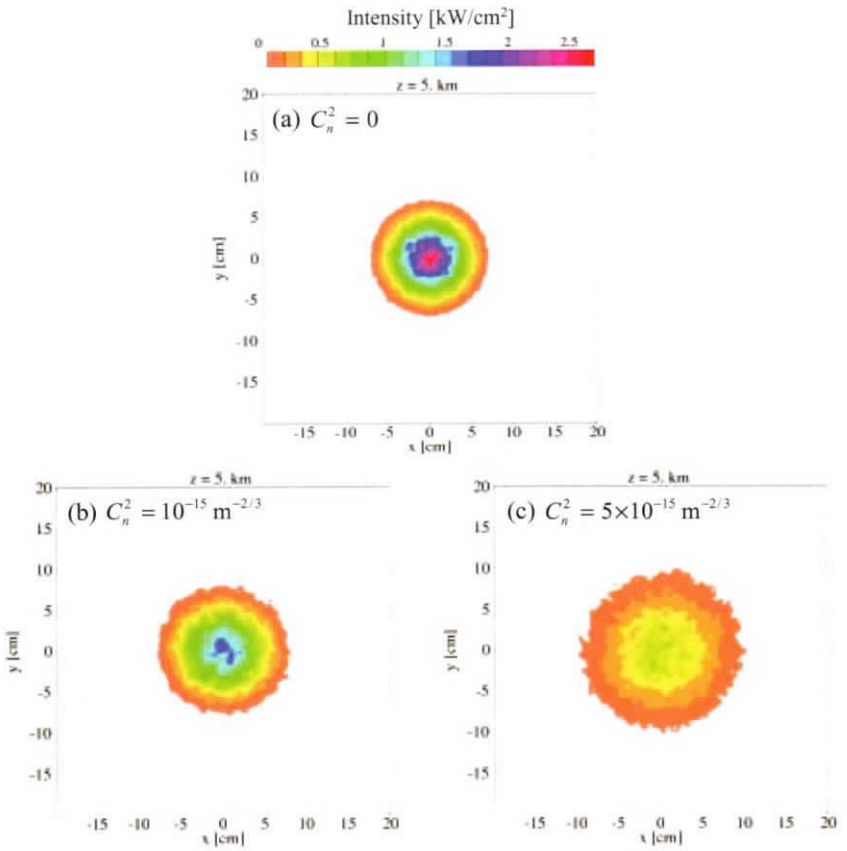

Fig. 9. Average intensity at the target plane ($L = 5$ km) for cases of (a) no atmospheric turbulence, (b) weak turbulence ($C_n^2 = 10^{-15}$ m$^{-2/3}$), and (c) moderate turbulence ($C_n^2 = 5 \times 10^{-15}$ m$^{-2/3}$) for the incoherent combining example of Fig. 6.

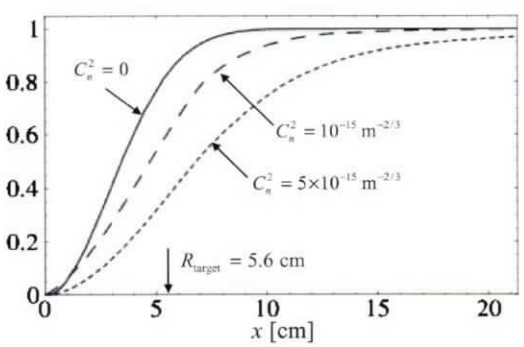

Fig. 10. Fractional power versus transverse coordinate x at a range of $L = 5$ km for the incoherent beam director of Fig. 6. Fractional power is defined as the power contained within a circle of radius x normalized to the total transmitted power. The radius of a circular target with an area of 100 cm^2 is $R_{target} = 5.6$ cm. Curves represent cases with no atmospheric turbulence, weak turbulence ($C_n^2 = 10^{-15}$ m$^{-2/3}$), and moderate turbulence ($C_n^2 = 5 \times 10^{-15}$ m$^{-2/3}$).

5. Discussion

We have presented a configuration for incoherently combining fiber lasers for long-range DE applications that can be implemented in the near term with commercially available fiber lasers. Our configuration uses recently developed, multikilowatt fiber lasers. These lasers, however, are not suitable for coherent beam combining because of their large linewidths and random phases. Coherent combining is limited to lower power fiber lasers and hence requires over an order of magnitude more fibers than the incoherent configuration.

A 20-kW, long-range (multikilometer) DE demonstration can be readily performed using present-day technology. This high-energy laser (HEL) demonstration would require ~10 fiber lasers, each producing ~2 kW of CW power. This system would require a beam director with a radius of ~13 cm and, excluding the power supply and cooling system, has a volume of ~6 m^3. The cost of the 10 fiber lasers is estimated to be $3 million. This near-term demonstration would address the important technical issue of controlling individual steering mirrors and the effects of tilt angle error and jitter. In addition, a successful long-range, HEL lethality demonstration would motivate further development of high-power fiber lasers for DE applications.

This incoherent beam combining configuration, in principle, is scalable to higher CW powers. For example, a 500-kW HEL system would require ~200 fiber lasers (2.5 kW/fiber) and have a beam director radius of ~65 cm, and the fiber lasers would occupy a volume of ~150 m^3.

6. Acknowledgments

This work was supported by the Office of Naval Research (ONR) and the Joint Technology Office. The authors appreciate useful discussions with Q. Saulter of ONR, L.N. Durvasula of DARPA, and J. Slater of Schaefer Corporation.

References

[1]Beland, R.R., "Propagation through Atmospheric Turbulence," in *The Infrared and Electro-Optical Systems Handbook*, vol. 2, edited by F.G. Smith, Environmental Research Institute of Michigan, Ann Arbor, MI, and SPIE Optical Engineering Press, Bellingham, WA (1993).

[2]Boullet, J., D. Sabourdy, A. Desfarges-Berthelemot, V. Kermène, D. Pagnoux, P. Roy, B. Dussardier, and W. Blanc, Opt. Lett. **30**, 1962 (2005).

[3]Bruesselbach, H., D.C. Jones, M.S. Mangir, M. Minden, and J.L. Rogers, Opt. Lett. **30**, 1339 (2005).

[4]Hecht, J., "Photonic Frontiers: High-Power Fiber Lasers: Pumping Up the Power," Laser Focus World, August 2005 (http://www.laserfocusworld.com).

[5]Jeong, Y., J. Nilsson, J.K. Sahu, D.B. Soh, P. Dupriez, C.A. Codemard, S. Back, D.N. Payne, R. Horley, J.A. Alvarez-Chavez, and P.W. Turner, Opt. Lett. **30**, 955 (2005).

[6]Loftus, T., A. Liu, P. Hoffman, A. Thomas, M. Norsen, R. Royse, and E. Honea, "Solid State and Diode Laser Tech. Review," BC-1, Albuquerque, NM, June 2006.

[7]Martin, J., "Simulation of Wave Propagation in Random Media: Theory and Applications," in *Wave Propagation in Random Media (Scintillation)*, edited by V.I. Tatarskii, A. Ishimaru, and V.U. Zavorotny, Society of Photo-Optical Instrumentation Engineers, Bellingham, WA (1993).

[8]Peng, Q., Z. Sun, Y. Chen, L. Guo, Y. Bo, X. Yang, and Z. Xu, Opt. Lett. **30**, 1485 (2005).

[9]Sprangle, P., J. Peñano, and B. Hafizi, "Optimum Wavelength and Power for Efficient Laser Propagation in Various Atmospheric Environments," NRL Technical Memorandum NRL/MR/6790-05-8907, 2005; also accepted for publication in J. Directed Energy.

[10]"Towards 100 kW Fiber Laser Systems- Scaling Up Power in Fiber Lasers for Beam Combining," Crystal Fibre A/S, White Paper, Feb. 28, 2006 (http://www.crystal-fibre.com/support/White_Paper_-_Towards_100kW_fiber_laser_systems_-_Scaling_up_power_in_fiber_lasers_for_beam_combining.pdf).

[11]Tünnermann, A., T. Schreiber, F Röser, A. Liem, S. Höfer, H. Zellmer, S. Nolte, and J. Limpert, J. Phys. B: At. Mol. Opt. Phys. **38**, S681 (2005).

[12]Washburn, B.R., S.A. Diddams, N.R. Newbury, J.W. Nicholson, M.F. Yan, and C.G. Jørgensen, Opt. Lett. **29**, 250 (2004).

[13]Wickham, M., "Coherently Coupled High-Power Fiber Arrays," presented at Photonics West 2006, San Jose, CA; Anderegg, J., S. Brosnan, E. Cheung, P. Epp, D. Hammons, H. Komine, M. Weber, and M. Wickham, SPIE **6102** (2006).

The Authors

Dr. Bahman Hafizi received B.Sc. and Ph.D. degrees in physics from Imperial College, London, in 1974 and 1978. He is president of Icarus Research, Inc. He was previously a Research Associate in the Department of Astro-Geophysics at the University of Colorado and a Staff Scientist for SAIC. His research areas include propagation of ultraintense laser pulses, laser-driven electron accelerators, laser–plasma interactions, nonlinear optics, advanced sources of electromagnetic radiation with application to imaging, lithography, and remote sensing. He is an Associate of the Royal College of Science and a member of the American Physical Society, the European Physical Society, and the IEEE.

Dr. Joseph R. Peñano received B.S. and Ph.D. degrees in plasma physics from the University of California, Los Angeles, in 1991 and 1998. He joined the NRL Beam Physics Branch in 2001. He conducts research on atmospheric propagation of ultrashort, high-intensity laser pulses for directed energy weapons and electronic countermeasure applications, advanced radiation sources, and laser-driven particle accelerators. He is the chief developer of HELCAP (High Energy Laser Code for Atmospheric Propagation). Prior to joining NRL, he held a National Research Council postdoctoral fellowship. He received the NRL Alan Berman Publication Award in 2003.

Dr. Phillip Sprangle received his Ph.D. in applied physics from Cornell University in 1973. He is Chief Scientist and Head of the Beam Physics Branch at NRL. His research areas include atmospheric laser propagation, free-electron lasers, and laser acceleration physics. Dr. Sprangle is a fellow of the American Physical Society, the IEEE, and the DEPS. He won the International Free Electron Laser Prize (1991), E.O. Hulburt Science and Engineering Award (1986), and Sigma Xi Pure Science Award (1994), as well as numerous publication awards. He has published more that 200 refereed scientific articles (28 letters) and holds 12 U.S. invention patents.

Dr. Antonio C. Ting received his Ph.D. degree in physics from the University of Maryland in 1984. He is a senior research physicist and the group leader of the High Field Physics Laboratory in the Plasma Physics Division of the Naval Research Laboratory. He conducts research on intense ultrashort pulse laser interactions with air, plasmas, and electron beams for directed energy weapons, standoff detections, electronic countermeasures, advanced x-ray sources, and particle accelerators. He is a Fellow of the American Physical Society and a member of Sigma Xi and the Directed Energy Professional Society.